Petroleum Science 19 (2022) 800–808

Contents lists available at ScienceDirect

Petroleum Science

journal homepage: www.keaipublishing.com/en/journals/petroleum-science

Original Paper

# Nanoparticle stabilized emulsion with surface solidification for profile control in porous media

Yi-Ning Wu [a, b], Xiang Yan [a, b], Ke Xu [c, **], Ruo-Yu Wang [d], Meng-Jiao Cao [a, b], Xiao-Da Wang [e], Yuan Li [a, b], Cai-Li Dai [a, b, *]

[a] Shandong Key Laboratory of Oilfield Chemistry, School of Petroleum Engineering, China University of Petroleum (East China), Qingdao, 266580, PR China
[b] Key Laboratory of Unconventional Oil & Gas Development, China University of Petroleum (East China), Ministry of Education, Qingdao, 266580, PR China
[c] Department of Energy and Resources Engineering, College of Engineering, Peking University, Beijing, 100871, China
[d] Dongxin Oil Production Plant, Shengli Oilfield Company, SINOPEC, Dongying, 257000, China
[e] College of Chemical Engineering, Fuzhou University, Fuzhou, 350116, China

ARTICLE INFO

*Article history:*
Received 17 December 2020
Accepted 3 September 2021
Available online 11 November 2021

Edited by Xiu-Qiu Peng

*Keywords:*
Nanoparticles
Emulsion stability
Flow behavior
Coalescence
Profile control

ABSTRACT

Profile control is utilized to redirect the injection water to low permeability region where a large amount of crude oil lies. Performed gel particles are the commonly used agent for redistributing water by blocking the pores in high permeability region. But the capability of deep penetration of performed gel particles is poor. Here, we formulate nanoparticle stabilized emulsion (NSE). The stability and the effect of NSE on the fluid redirection in a three-dimensional porous medium were investigated. By using μ-PIV (particle image velocimetry), it was found that the velocity gradient of continuous fluid close to the nanoparticle stabilized droplets is much higher than that close to surfactant stabilized droplets. NSE behaves as solid particle in preferential seepage channels, which will decrease effectively the permeability, thereby redirecting the subsequent injection water. Furthermore, NSE shows high stability compared with emulsion stabilized by surfactant in static and dynamic tests. In addition, water flooding tests also confirm that the NSE can significantly reduce the permeability of porous media and redirect the fluid flow. Our results demonstrate NSE owns high potential to act as profile control agent in deep formation.



## 1. Introduction

With continued demand for oil and gas, the methods that can extend the life of mature oilfields are needed urgently. The major parameter that affects oil recovery unfavorably is excessive water production which mainly results from viscous fingering caused by the huge viscosity difference between displacing phase and displaced phase such as water and crude oil. Besides, formation permeability heterogeneity exacerbates the channeling of the displacing fluid (Saikia et al., 2020). Herein, Enhanced oil recovery (EOR) techniques are of paramount importance for mature oilfields (Bai et al., 2015). All kinds of methods have been proposed to reduce excessive water production in oil wells, like gel treatment, polymer flooding, alkaline-surfactant-polymer flooding (ASP), emulsion flooding, and so on (Liu et al., 2010). Polymer gel is preferentially used as a profile control agent to plug high permeability paths, diverting the fluid into low permeability zones (Zhao et al., 2015). Nevertheless, the polymer used to form gel is always polyacrylamide which would degrade or lose the thermal stability in high temperature formation, leading to a declining plugging efficacy (Saikia et al., 2020; Samuelson et al., 1996; Caulfield et al., 2002). In addition, due to the strong shear stress cause by porous media, the dispersed particle gel (DPG) may reduce its gel strength and can't function as an in-depth fluid diversion agent.

Emulsion, an important oil-water two-phase system, has been widely studied and used in many fields such as chemistry (Yin et al., 2013), food industries (Xiao et al., 2016), materials science (Wang et al., 2018) and oil recovery (Perino et al., 2013; Sharma et al., 2014; Wu et al., 2017) because of their special physicochemical

* Corresponding author. Shandong Key Laboratory of Oilfield Chemistry, School of Petroleum Engineering, China University of Petroleum (East China), Qingdao, 266580, PR China.
** Corresponding author.
*E-mail addresses:* kexu1989@pku.edu.cn (K. Xu), daicl@upc.edu.cn (C.-L. Dai).

https://doi.org/10.1016/j.petsci.2021.11.001

**Nomenclature**

| | |
|---|---|
| Postscript | In order to facilitate the understanding of the acronyms in this article, here is a summary of the acronyms used frequently in this article |
| NSE | nanoparticle stabilized emulsion |
| NS | nano-silica |
| DTAB | Dodecyl Trimethyl Ammonium Bromide |
| NS-DTAB | the complexes of nano-silica and DTAB |
| SDS | Sodium Dodecyl Sulfate |
| PIV | particle image velocimetry |

and flow properties (Yu et al., 2019). Especially in oil recovery field, O/W emulsion owns high apparent viscosity and low surface tension with oil relative to water, which make it easier for emulsion to penetrate into deep formation and small pores because the capillary force needed to be overcome become smaller (Wang et al., 2006; Shi et al., 2014). On the other hand, the droplets can cause pore blockage due to the Jamin effect, creating flow path diversion away from the wellbore (McAuliffe, 1973; Ponce F et al., 2014), and therefore the emulsion can act as displacing fluid and fluids diverting agent to enhance oil recovery.

Surfactant is a commonly used emulsifier, which can reduce the interfacial tension (Bera et al., 2013; Almobarky et al., 2017) and the required energy for emulsification (Forgiarini et al., 2001), decreasing the degree of instability of emulsion. Nevertheless, the disadvantages of surfactant are also notable. The adsorption of surfactant at oil-water interface is always in a state of dynamic balance because of its low desorption energy (Guo et al., 2016; Paulson and Pugh, 1996; Matteo et al., 2012; Kong et al., 2010), which means that surfactants are easy to detach from oil-water interface. As a result of that, during the transportation process of emulsion in formation, the effective concentration of surfactant in the emulsion system will gradually decrease due to the adsorption of surfactants on rock surface and the dilution of formation water (Yang, 1985), making the emulsion become more unstable. Therefore, emulsion stabilized by surfactant alone have a short stability period.

In comparison, emulsion stabilized by nanoparticles have better stability due to the high desorption energy (Aveyard et al., 2003; Binks. 2002; Du et al., 2010; Curschellas et al., 2012; Metin et al., 2012), which means that nanoparticles can adsorb firmly at oil-water interface. Pickering et al. took the lead in using small particles instead of surfactant to stabilize emulsion (Pickering, 1907). Afterwards, Binks and Lumsdon, 2000 carried out a series of investigations on nanoparticles stabilized emulsion and found that the stability of which is mainly affected by the interfacial property of nanoparticles (Binks and Clint, 2002; Binks. 2001; Binks et al., 2002). The adsorption of nanoparticles at oil-water interface also requires amphiphilicity. Thus, in order to modify the interfacial property of nanoparticles, two category methods have been proposed. One method is surface grafting realized by endowing nanoparticle surface with hydrophilic and hydrophobic functional groups coinstantaneously (Dendukuri et al., 2007; Walther et al., 2008; Saigal et al., 2010; Alvarez et al., 2012). The other method is physical modification through electrostatic interaction, hydrogen bond and so on (Wu et al., 2019; Alyousef et al., 2018; Liu et al., 2017; Toor et al., 2018). It is obvious that physical modification is simple and feasible. Binks and Lumsdon, 2000 investigated the behavior of emulsions stabilized by a mixture of silica nanoparticles and cationic surfactant under different pH, and revealed that the presence of surfactant altered the surfactancy of NPs (Binks et al., 2007).

Additionally, it has been found that nanoparticles could form a solid-like film on the gas-liquid surface, which would decrease the contact area of gas-liquid and prevent the foam from Ostwald ripening (Wu et al., 2018). To further illustrate how surfactant decorated nanoparticles affect bubble flow behaviors, Yu et al. investigated the differences between interfacial properties of bubble with various stabilizers by measuring the flow field of continuous phase around bubble surface using particle image velocimetry (PIV) (Yu et al., 2019). They found that the continuous phase velocity in the case where nano-silica (NS)-surfactant complexes were added was much smaller than the case using pure surfactant, and therefore the bubble surface showed a better fluidity in the system using surfactant alone. It was the solid-like films formed by NS at the gas-liquid interface that made bubble behave as a solid wall. Based on the discoveries above, we speculate whether there would be similar phenomena and mechanisms in NSE.

With such conjecture, a novel system was proposed to stabilize emulsion in this research. Dodecyl trimethyl ammonium bromide (DTAB) was chosen as the modifier to change the surfactancy of nano-silica through electrostatic interaction. The aim of this work is to thoroughly explore the flow behavior of emulsions stabilized by different emulsifiers (surfactants with or without NS), and the properties of which under shear force were further investigated. In addition, the profile control capacity of emulsions stabilized by different emulsifiers in porous media will also be studied.

## 2. Materials and methods

### 2.1. Materials

Dodecane (98% of purity) from Aladdin Biochemical Technology Co., Ltd (Shanghai, China) was used as oleic phase for emulsification. Nano-silica (NS) (LUDOX® HS-30 colloidal silica, 30 wt%) was purchased from Sigma-Aldrich with a surface area of 220 $m^2\ g^{-1}$, pH of 9.8 and a density of 1.21 g $mL^{-1}$. Dodecyl trimethyl ammonium bromide (DTAB) and sodium dodecyl sulfate (SDS) were obtained from Sinopharm Group Chemical Reagent Co., Ltd. Ultrapure water was prepared by using reverse osmosis unit (ULUPURE, UPT–II–5T). The red fluorescent polymer microspheres from Thermo Scientific function as tracer agent in the flow field measurement experiments. In the oil displacement experiments, the diameter of quartz sand is of 50 mesh.

### 2.2. Microfluidic devices

The layout of the microfluidic device used in the experiments is shown in Fig. 1. The channel was mechanically milled on a polymethyl methacrylate (PMMA) plate (190 × 120 × 8 mm). The microchannel structure consists of a droplet-formation section, a snail-like section, and an expanding chamber. The droplet-formation section is used to generate oil droplets. Snail-like section is designed to guarantee enough retention time in microchannel, thereby providing abundant time for nanoparticle adsorption. The dispersed phase, dodecane was injected to the micro device from point B at a flow rate of $Q_1$ (0.03 mL·$min^{-1}$-0.1 mL $min^{-1}$) and the aqueous phase was injected to the micro device from point A at a flow rate of $Q_2$ (0.1 mL·$min^{-1}$-1 mL $min^{-1}$), then the aqueous phase bifurcate into two branches vertical to the oil injection channel. The droplet-formation and snail-like sections have the same cross section, whose width ($W$) and height ($H$) are both 400 μm. The expanding chamber width ($W_e$) and height ($H_e$) are 1800 μm and 400 μm, respectively.

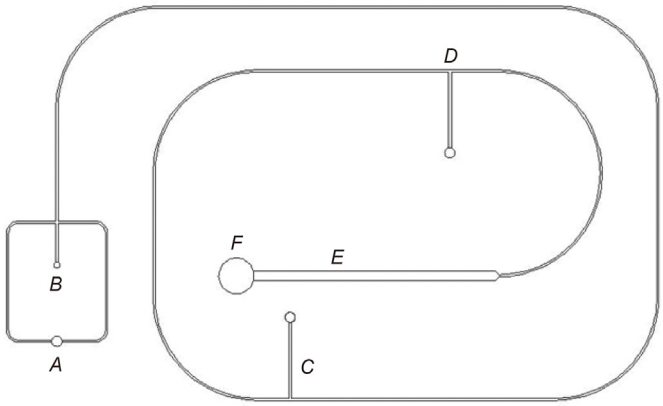


**Fig. 1.** Microfluidic devices (**a**) continuous phase inlet, (**b**) oil phase inlet, (**c**) oil entrapment structure, (**d**) entrance of oil entrapment structure, (**e**) expanding chamber, (**f**) main outlet.

### 2.3. Methods

#### 2.3.1. Preparation of emulsions

The DTAB solutions, SDS solutions and NS-DTAB dispersions were prepared respectively. For DTAB solutions and SDS solutions, a certain amount of DTAB or SDS and ultra-pure water were added and mixed in the beaker. To prepare 100 g 8 mmol $L^{-1}$ SDS solution, 0.2307 g SDS was first added into the beaker, followed by 99.7693 g ultra-pure water, and then the solution was mechanically stirred for at least 1 h to thoroughly dissolve SDS in water. The steps of pure DTAB solution preparation were similar to the steps above, and the only difference between them was the dosage of the used chemical agent. For NS-DTAB dispersion, DTAB was first added to the beaker followed by the addition of water, and then NS were added dropwise into DTAB solution. Ultrasonic dispersion method was used for more than 10 min to ensure homogeneity. Last, an equal volume of DTAB solutions, SDS solutions and NS-DTAB dispersions were mixed with dodecane, respectively using homogenizer with agitation speed set at 10000 rpm for 5 min. The generated emulsions were used for further investigation.

#### 2.3.2. Diameter and zeta potential of NS

A Nano Brook Omni instrument (Brookhaven Instruments Corporation) was used to measure the diameter and zeta potential of nano-silica with different DTAB concentration. The temperature was set at 25 °C.

#### 2.3.3. Flow visualization

Micro-particle image velocimetry (μ-PIV) from LaVision. Ltd was used to perform quantitative measurements on the flow fields surrounding single droplet and numerous oil droplets. The whole flow field measurements experiments were performed on the microfluidic device and the flow visualization experiments setup is shown in Fig. 2. The velocity vectors were calculated by a conventional cross-correlation PIV algorithm. The μ-PIV instrument was used to measure the flow field of continuous phase around oil droplet surface with the focal plane of μ-PIV located in the middle of the channel in the vertical direction so as to further illustrate the influence of NS-DTAB complexes on oil droplets' flow behaviors. For these experiments, single oil droplet was first generated in the droplet-formation section. Afterwards, different continuous phase, as NS-DTAB complexes dispersions, DTAB or SDS solution, was injected separately at a flow rate of 1 mL $min^{-1}$ to drive the oil droplet entering the expansion chamber as shown in Fig. 1. After the droplet entered the expansion chamber, the flow rate of continuous phase was reduced to a rate much lower than 1 mL $min^{-1}$ for the purpose of avoiding that the rate was too high to flush away the droplets, and then maintained to further test the flow field around the droplet. The measurement method of the flow field surrounding multiple droplets was similar to the steps above, the only difference between them was that single droplet was replaced by numerous droplets.

In addition, the homogenous micromodel was used to measure the permeability after the micromodel was full of emulsion to further confirm the validity of the conclusions drawn from the PIV experiments. The procedures were as following: 1. The permeability of the micromodel was measured first using Darcy's law: $K = \frac{Q\mu L}{A\Delta P}$ by water flooding at a flow rate of 0.5 mL $h^{-1}$, and the $\Delta P_0$ was gained; 2. Fill the micromodel with 10 mmol $L^{-1}$ DTAB stabilized emulsion, and then the 10 mmol $L^{-1}$ DTAB solution was used to flow through the micromodel at the flow rate of 80 μL $h^{-1}$ to prevent the emulsion from being displaced out at a high flow rate, measure the pressure drop as a function of time; 3. After the measurement was finished, clean up the micromodel, and measure the permeability at the flow rate of 0.5 mL $h^{-1}$ again, gain the $\Delta P_1$; 4. Inject the same volume of NS-DTAB emulsion (0.6 mmol $L^{-1}$ DTAB with 2 wt% NS) as DTAB stabilized emulsion. Then the 0.6 mmol $L^{-1}$ DTAB with 2 wt% NS dispersion was used to flow through the micromodel at the same flow rate of 80 μL $h^{-1}$, measure the pressure drop with time; 5. Repeat step 3, and gain $\Delta P_2$; 6. Clean up the micromodel and inject the same volume of 8 mmol $L^{-1}$ SDS emulsion. Then the 8 mmol $L^{-1}$ SDS solution was used to flow through the micromodel at the same flow rate of 80 μL $h^{-1}$, measure the pressure drop with time; 7. Repeat step 3, and gain $\Delta P_3$.

#### 2.3.4. Microscopic experiments

Coalescence experiments and microscopic images were investigated in this section. In coalescence experiments, surfactant solutions or silica NPs dispersions were first added to a square glass container and then dodecane was added to the container slowly to form an oil-water interface. The needle connected to a syringe was immersed in the surfactant solutions or silica NPs dispersions. The volume of oil droplet was controlled by adjusting the flow rate of the pump. As the droplet volume increased, oil droplet came into contact with the oil-water interface and then the oil droplets coalesced with the oil in the square glass container. The process of coalescence was recorded by Photron Fastcam SA-Z high speed camera which can be also used to capture the microscopic images of droplets in the emulsions stabilized by different emulsifiers and the images were uploaded to the software to be further processed. The microscopic images served as evidence for the coalescence experiments. In addition, a Leica DMi8 C inverted microscope was used to observe the morphology of droplets in emulsions. Average sizes of oil droplets in the emulsions stabilized by different emulsifiers were recorded at 10 min, 1 d, 2 d, 3 d, 4 d, 6 d, 8 d, 12 d, 20 d and 1 month after emulsion preparation.

#### 2.3.5. Rheological properties of emulsions

The rheological properties are crucial parameters to assess the stability of emulsion. Rheological measurements were employed by the Haake RS6000 rheometer with a cone-and-plate sensor system. For steady shear measurement, the viscosities of emulsions were recorded as the shear rates ranging from 0.01 to 100 $s^{-1}$. In oscillatory measurements, storage modulus and loss modulus of emulsion were investigated at the rotational speed ranged from 0.01 to 100 rad $s^{-1}$. The experimental temperature was set at 25.00 ± 0.05 °C.

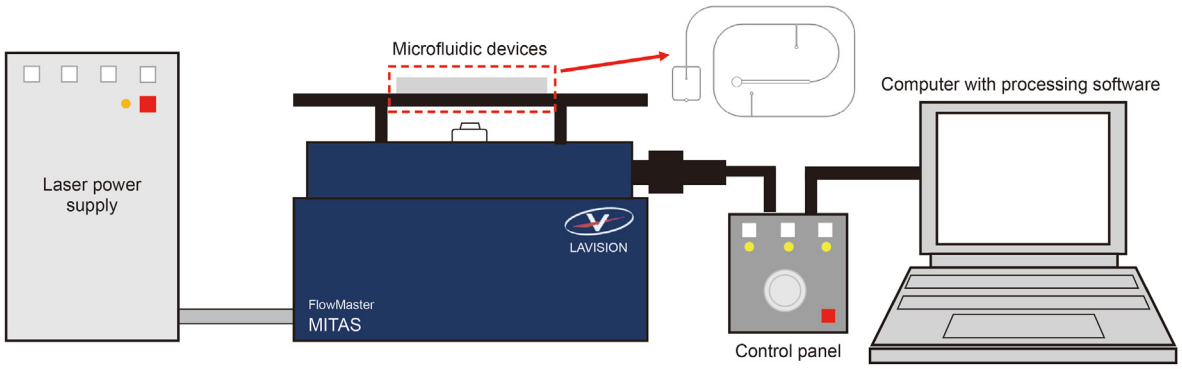


**Fig. 2.** Schematic diagram of the flow visualization experiments setup. The whole flow visualization experimental setup is composed of laser power supply, CCD camera, control panel and computer with processing software.

*2.3.6. Dynamic displacement tests*

The oil displacement experiments were performed using sand pack to study the profile control capability of emulsion at secondary water flooding stage.

The experimental procedures are as following: (1) The sand pack was first filled with dry sand and then saturated with brine slowly with successive compaction. (2) The pore volume of sand pack was determined by the volume of used brine when the sand pack was full. (3) The permeability of sand pack was measured using Darcy's law: $K = \frac{Q\mu L}{A\Delta P}$ by brine water flooding at the flow rate of 1.0 mL min$^{-1}$, where $Q$ is the flow rate, $\mu$ is the viscosity of the brine water, $L$ is the length of sand pack, $A$ is the cross-sectional area of sand pack, $\Delta P$ is the injection pressure of water flooding. After that, sand pack was displaced with oil at a flow rate of 0.1 mL min$^{-1}$ until no more water was produced. (4) Water flooding stage was carried out at a flow rate of 1.0 mL min$^{-1}$ until the water cut reached 98%. Subsequently, 0.1 pore volume (PV) emulsion was injected into the sand pack with same pump rate. Afterwards, secondary water flooding was continued until the water cut approached 98% again. The volume of oil and produced fluid were recorded every 1 min. In the meantime, the pressure drop across the rock samples was measured. The total recovery was the ratio of the volume of total produced oil and initial saturated oil. The schematic diagram of macroscopic dynamic test in sand-packs is shown in Fig. 3.

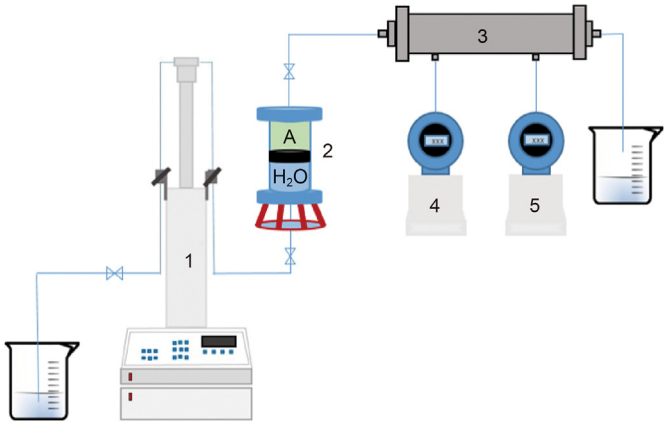


**Fig. 3.** Schematic diagram of water flooding test in sand-packs (1. micro pump; 2. intermediate container, where A is filled with water or emulsion; 3. sand-packs; 4–5. Rosemount pressure gauge).

## 3. Results and discussion

### 3.1. Interfacial property of NS-DTAB complexes at oil-water interface

Based on the conjecture mentioned at the end of the introduction, the mechanisms for diverting subsequent injected water of NSE were proposed: The adsorption of NS-DTAB complexes at oil-water interface would result in interface hardening, forming a solid-like film, and the solid-like film could increase the flow resistance of injection water that flows through the oil-water interface to a great extent, which endows the emulsion with better plugging ability to achieve the in-depth profile control.

The choice of suitable DTAB concentration range in the presence of NS was discussed in the Supporting Information S1. The physical properties of NS-DTAB dispersion were measured first, and the results verified the adsorption of DTAB molecules on the surface of NS by electrostatic attraction (Supporting Information S2.).

To directly investigate the effect of NSE interfacial properties on the flow field, a micromodel containing snail-like section and expanding chamber was used and the flow fields surrounding the nanoparticle stabilized droplets were recorded and analyzed by μ-PIV and accessory software LaVision DaVis 8 as well. As shown in Fig. 4, when the emulsion is stabilized by NS-DTAB complexes, the continuous phase velocity close to droplet surface is much smaller than central maximum velocity. The fluidity of droplet surface in emulsion with the NS-DTAB complexes is significantly less than the droplet stabilized by DTAB or SDS alone. Furthermore, the continuous phase velocity close to droplet surface decreased with the increase of DTAB concentration in NS-DTAB dispersion. This also represents that the packing density and stability of NS-DTAB complexes at oil-water interface would increase with the improvement of NS amphiphilicity, further resulting in the increase of velocity gradient at droplet surface. We compared the velocity distributions in y = 0 from five different systems as shown in Fig. 4g (for convenience, the x = 0 was reset at oil droplet surface). The velocity gradient in NS-DTAB systems is larger than the system containing DTAB or SDS alone. In addition, the increase of DTAB concentration in NS-DTAB dispersion led to the augment of velocity gradient as shown in Fig. 4. These phenomena imply that the adsorption of NS-DTAB complexes at oil-water interface would result in interface hardening, forming a solid-like film. NSE played the role of solid particle in preferential seepage channels. The droplet with solid-like film could reconstruct the channeling-path and convert small fracture into porous media again as shown in Fig. 5. In addition, it could be seen that the droplets in SDS system easily coalesced when emulsion was subjected to water flooding while this phenomenon hardly appeared in NSE from Fig. 5, which means that the anti-flush ability of SDS stabilized emulsion is worse than NSE.

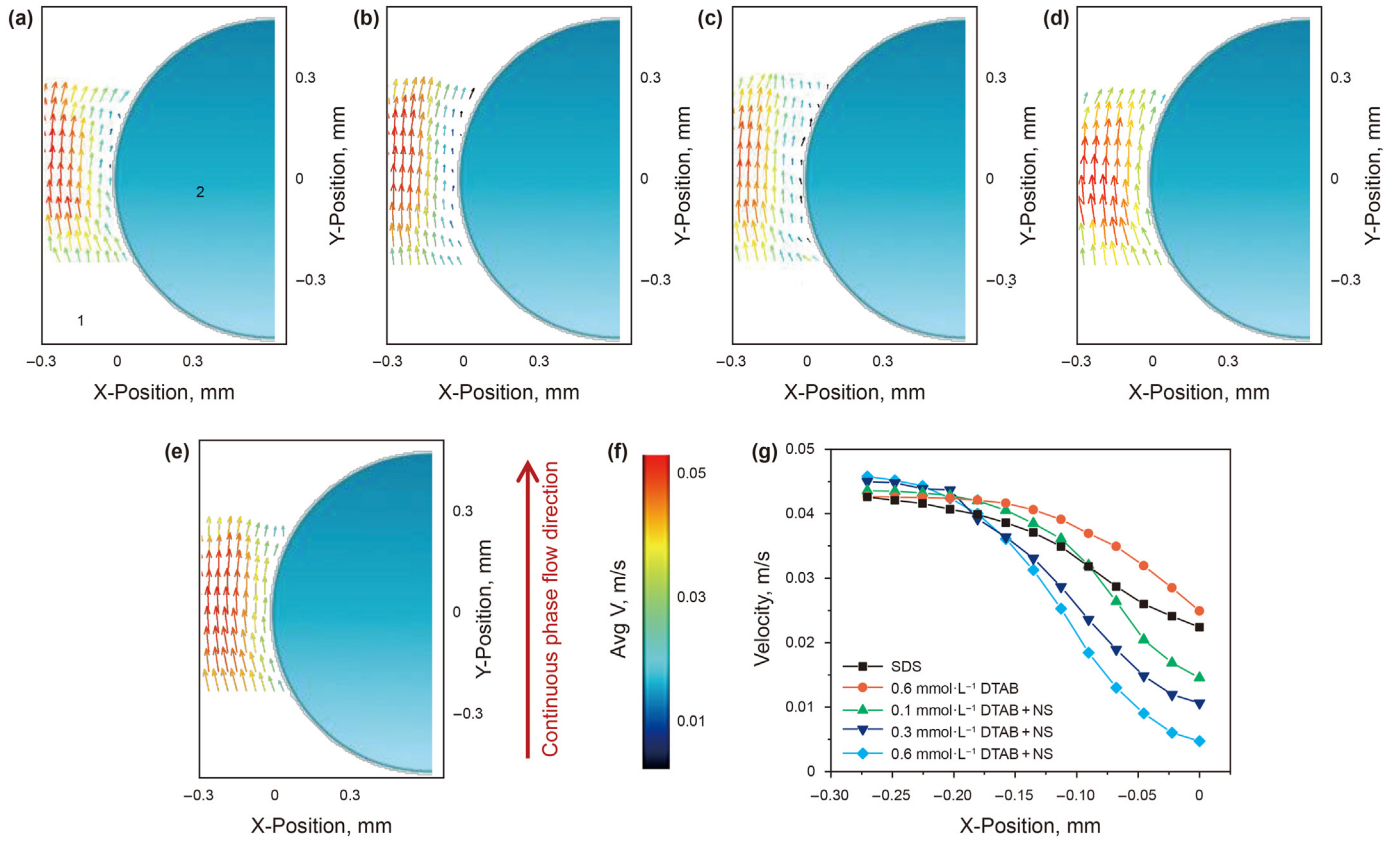


**Fig. 4.** The flow field surrounding single droplet (**a**) 0.1 mmol $L^{-1}$ DTAB with 2 wt% NS dispersion (1: continuous phase, 2: oil droplet); (**b**) 0.3 mmol $L^{-1}$ DTAB with 2 wt% NS dispersion; (**c**)0.6 mmol $L^{-1}$ DTAB with 2 wt% NS dispersion; (**d**) 0.6 mmol $L^{-1}$ DTAB; (**e**) 8 mmol $L^{-1}$ SDS; (**f**) velocity bar; (**g**) velocity distributions in y = 0 from five different systems.

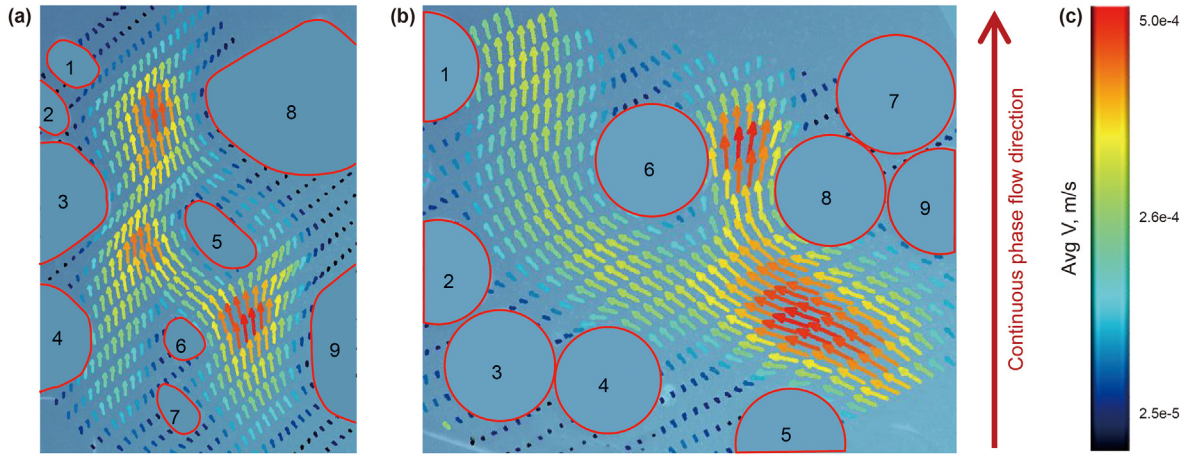


**Fig. 5.** The flow field surrounding numerous droplets (**a**) 0.6 mmol $L^{-1}$ DTAB with 2 wt% NS dispersion (1–9: oil droplets); (**b**) 8 mmol $L^{-1}$ SDS (1–9: oil droplets); (**c**) velocity bar.

Consequently, NSE weakens the degree of formation heterogeneity, diverting the following water into relatively low permeability zones, increasing the sweep efficiency and finally enhancing the oil recovery.

### 3.2. Relationship between flow field and pressure drop in homogenous micromodel

To confirm that the anti-flush ability of the NS-DTAB stabilized emulsion is better than the emulsion stabilized by surfactant alone, the interrelation between the pressure drop of different solutions flowing through the homogenous micromodel after the model was full of corresponding emulsion and flow fields was investigated individually.

As depicted in Fig. 6, the pressure drop increased continually with time. Besides, the pressure drop of the NS-DTAB system increased more quickly and was much higher all the time, in comparison with the cases using the DTAB and SDS. After 2 h, the pressure drops for the three systems were 0.26 kPa, 0.15 kPa, and 0.09 kPa, respectively. It is obvious that the NS-DTAB system has

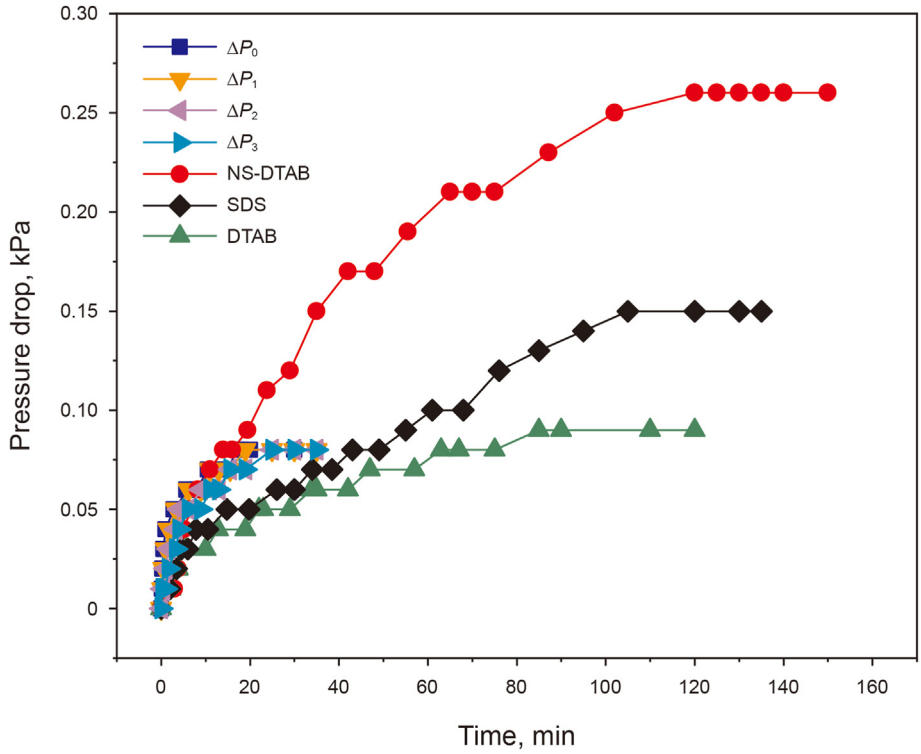


**Fig. 6.** Pressure drop measurements of the homogenous micromodel after the model was injected with different emulsions (10 mmol $L^{-1}$ DTAB stabilized emulsion, 0.6 mmol $L^{-1}$ DTAB with 2 wt% NS stabilized emulsion and 8 mmol $L^{-1}$ SDS stabilized emulsion).

more powerful resistance to water invasion, resulting in a larger pressure drop, which is caused by the interface hardening.

Combining with the flow fields of the three systems, the fluidity of the NS-DTAB system was less than the surfactant stabilized system so that the NS-DTAB system could generate a larger flow resistance. Consequently, at the same flow rate, a larger pressure drop occurs for the NS-DTAB system relative to that of the DTAB and SDS system in the homogenous micromodel. Besides, the $\Delta P_0$, $\Delta P_1$, $\Delta P_2$, and $\Delta P_3$ were almost the same, 0.08 kPa, proving that the variation in pressure drop was caused only by the temporary emulsion plugging instead of the permanent permeability loss under the circumstance of the micromodel being cleaned completely and no substance left in the previous measurements.

### 3.3. Emulsion stability

From the results above, we speculate that the solid-like film formed at interface at micro scale would affect some macroscopic properties of NSE like shear viscosity, elastic modulus and viscous modulus. Therefore, in this section, the static and dynamic stability of emulsions stabilized by different emulsifiers were investigated.

#### 3.3.1. Static stability

The volume of emulsion was recorded after surfactant solution or nanoparticle fluid was emulsified with dodecane. The rate of volume shrinkage of emulsion was chosen to evaluate the static stability. Fig. 7a shows the changes in the volume of emulsions stabilized by different emulsifiers with time. The inset in Fig. 7a showed the evolution of DTAB stabilized emulsion: emulsion volume reduced with time, which might be attributed to the coalescence of droplets. A small amount of water phase was also observed at the bottom of the glass bottle after 30 min. However, there was no obvious change in NSE volume after 7 days, indicating that NSE displayed outstanding stability for months. As indicated by Fig. 7a, the volume of NS-DTAB stabilized emulsion was approximately 3 times and 12 times as much as that of DTAB and NS stabilized emulsion after 20 days, respectively.

From Fig. 7b, the average size of droplets in the emulsion stabilized by NS-DTAB was almost as same as that in emulsion using SDS just after preparation. But the average size of droplets in the emulsion stabilized by SDS continually increased with time, which might be ascribed to the coalescence of droplets. When droplets collide with each other, coalescence process might happen to reduce interface free energy of the system. Surfactant molecules originally adsorbed at oil-water interface could rearrange or enter the aqueous phase when the coalescence occurred due to low desorption energy. However, after the 6th day of preparation, the average size of droplets in the NS-DTAB stabilized emulsion hardly changed. The shape of droplets which were observed from the microscopic images was not a regular circular, but a non-equilibrium shape, such as dumbbell-shape and gourd-shape. Besides, wrinkles can be clearly observed on the surface of some droplets. This special phenomenon proves that there might be a film which was formed by the adsorption of NS-DTAB at oil-water interface. As coalescence processes proceed, NS-DTAB complexes will not desorb from oil-water interface due to high desorption energy, and the interface coverage increase. When the interface is occupied completely, droplets coalescence processes will be suspended in NSE. The results of oil droplets coalescence process in different solutions or dispersions again confirmed the validity of these conclusions (Supporting Information S3.).

#### 3.3.2. Rheological stability

The rheological properties of emulsions were studied as indicators of dynamic stability. The process of emulsion's being subjected to shear force simulates the flow of emulsion through

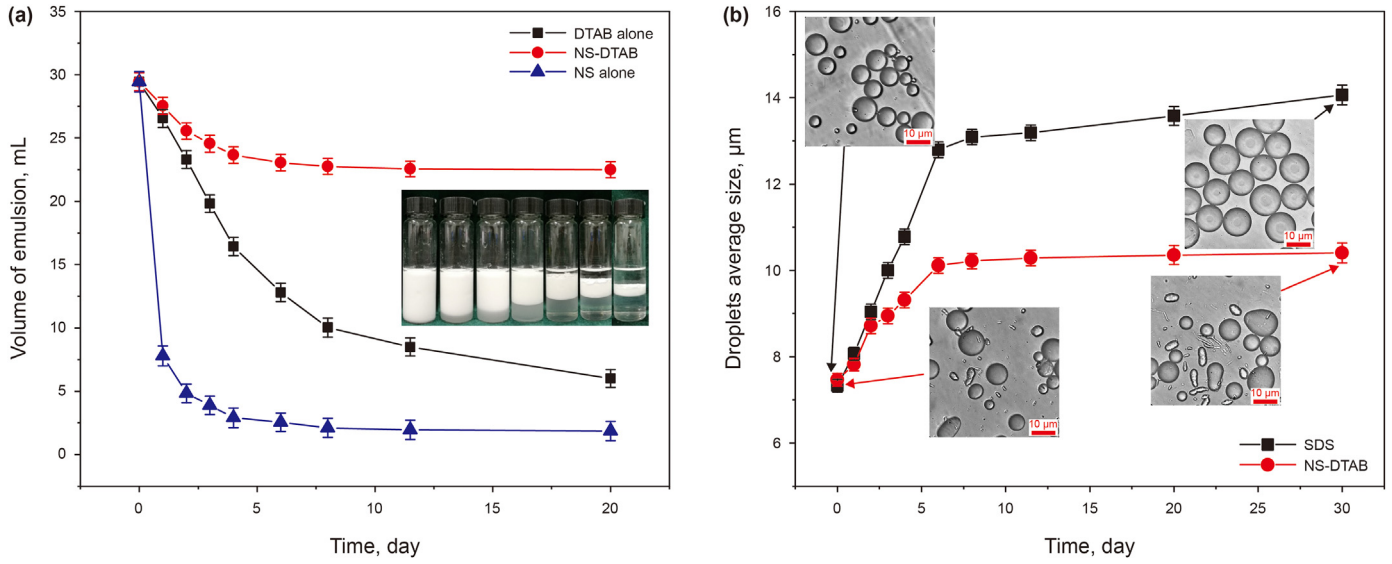


**Fig. 7.** (**a**) The volume of emulsions stabilized by different emulsifiers (10 mmol $L^{-1}$ DTAB solution (inset picture: 0, 1 d, 2 d, 3 d, 6 d, 11 d and 20 d from left to right), 0.5 mmol $L^{-1}$ DTAB with 2 wt% NS dispersion and 2 wt% bare NS) with time. (**b**) Average size of droplets in the emulsions stabilized by (1) 8 mmol $L^{-1}$ SDS solution (2) 0.6 mmol $L^{-1}$ DTAB with 2 wt% NS dispersion with time.

pore-throat structure. The rheology of emulsions stabilized by different emulsifiers (surfactant solution or NS-surfactant dispersions) were researched in this section. First, emulsions were prepared to perform the tests that varied DTAB concentrations by fixing the concentration of NS (2 wt%). It was difficult to produce emulsion when DTAB concentration was 0.01 mmol $L^{-1}$, while emulsions volume could maintain at a similar level after they were just prepared when DTAB concentration was 0.05, 0.1, 0.2, 0.3, 0.4, 0.5, 0.6 or 0.7 mmol $L^{-1}$. As shown in Fig. 8a, shear viscosity of emulsions stabilized by different emulsifiers changed with shear rate. Different emulsions showed the same trend: the shear viscosity of emulsion declined with rising shear rate. At the same shear rate, the viscosity for the cases where the silica nanoparticles were added was always higher relative to the system using DTAB and SDS surfactant alone. The increase of emulsion viscosity could simultaneously help to suppress the coalescence of droplets in the emulsion. At fixed silica nanoparticles concentration, the addition of DTAB from low to high concentrations could obviously produce steadier emulsions than DTAB by itself. Oscillatory measurements were also conducted to study the emulsions stability and results are shown in Fig. 8b. The changing process in storage modulus (G′) and loss modulus (G″) with rotational speed ($\omega$) was recorded. Emulsion using DTAB alone displayed low viscoelastic properties at low rotational speeds, which indicated the instability of emulsion at low rotational speeds. Storage modulus and loss modulus increase with the increment of rotational speed, meaning that emulsion gradually reaches a relatively steady state. Differently, the storage modulus and loss modulus of emulsions stabilized by NS-DTAB hardly changed with time, and the elastic modulus were always higher than viscous modulus while elastic modulus of DTAB and SDS stabilized emulsions were lower than viscous modulus in the most of time, confirming the speculation that interface hardening could effectively strengthen the stability of NSE. It is the solid-like film that endows the NSE with special properties, making NSE

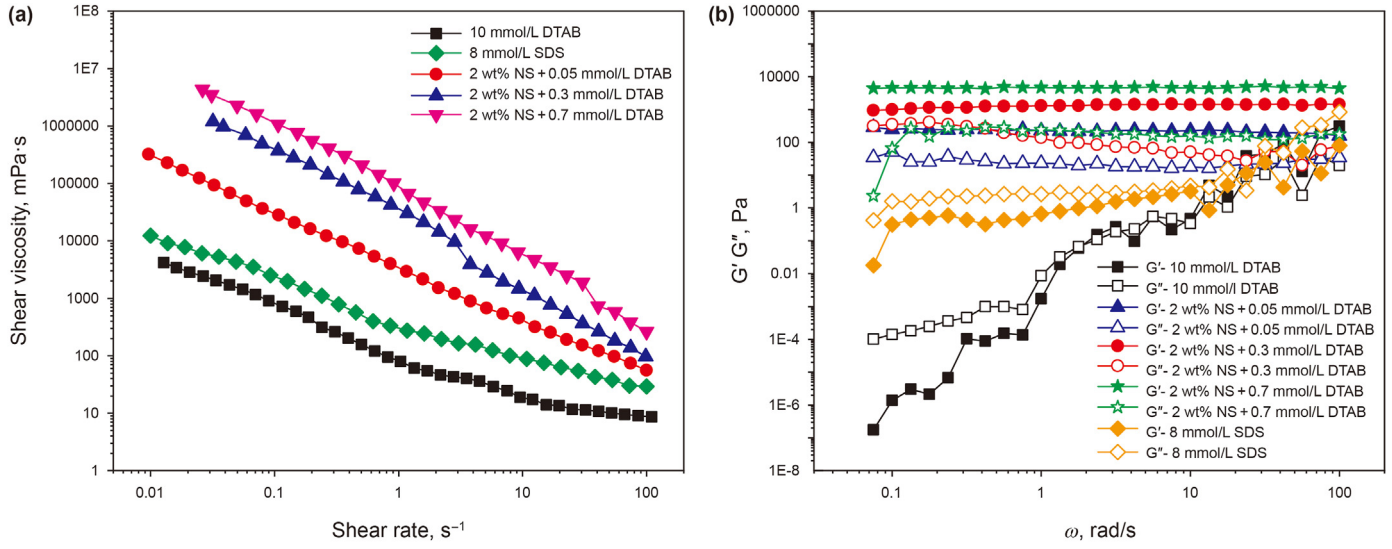


**Fig. 8.** (**a**) Steady shear measurement and (**b**) Oscillatory measurement results of emulsions stabilized by different emulsifiers.

**Table 1**
Recovery in different stages of displacement oil.

| Sand pack number | Permeability (D) | Recovery during initial water flooding stage, % | Recovery during subsequent water flooding stage, % | Accumulated Recovery, % |
|---|---|---|---|---|
| a | 2.436 | 58.57 | 22.14 | 80.71 |
| b | 2.811 | 59.42 | 10 | 69.42 |

show a greater elasticity relative to the emulsion using DTAB alone. So the NSE could behave more like a solid to be resistant to the deformation, which means that it is more difficult for droplets in NSE to flow through the pore throat structure and therefore the NSE has better plugging ability. Same as the trend of the shear viscosity, storage modulus and loss modulus of emulsion increase as the surfactancy of NS increases, indicating that the emulsion stability improved as DTAB concentration increased. In summary, the properties of emulsion were indeed affected by the presence of solid-like film, suppressing the coalescence of droplets effectively and making emulsion have remarkable anti-shear ability.

### 3.4. Nanoparticle stabilized emulsion (NSE) for enhanced oil recovery in porous media

To investigate the properties of NSE in enhanced oil recovery in 3 dimensional porous media, two comparative tests of oil displacement were carried out using emulsion stabilized by SDS (SDS concentration was of 8 mmol $L^{-1}$) and emulsion stabilized by nanoparticle with surface activity (the complex formed by 2 wt% NS and 0.6 mmol $L^{-1}$ DTAB). The oil recoveries in different stages of the two tests are summarized in Table 1. The permeabilities of two sand packs were 2.436 $\mu m^2$ and 2.811 $\mu m^2$, respectively. In the experiments, the pressure drop was regarded as an indicator to evaluate the stability of emulsion.

In Fig. 9, the injection pressure is plotted with respect to the injection volume. During the subsequent water flooding stage, the pressure drop produced by NS-DTAB stabilized emulsion rose more quickly than the SDS stabilized emulsion. Comparing the difference value of the highest pressure drop between subsequent water flooding stage and first water flooding stage, the NS-DTAB and SDS systems were 10.358 kPa and 4.088 kPa, respectively. It can be seen that the difference value of NS-DTAB systems was almost twice that of the SDS system. The enhancement of pressure drop means that there exists an obvious decline in the permeability of sand pack, which is caused by the emulsion plugging preferential channels, and then the water is diverted into low-permeability zones. We also observed a trend during the subsequent water flooding stage: In the beginning, the pressure drop increased quickly, but then started to descend after reaching the maximum value. The pressure drop of SDS system descended sharply while that of NS-DTAB system descended a little, and the value of pressure reached a stable state after the transient decline. The sharp decline of SDS system pressure drop results from the structure destruction of a part of the emulsion, which in turn illustrates the worse stability of SDS system compared with NSE when emulsion is subjected to water invasion. The higher the pressure, the steadier the emulsion, meaning more powerful resistance that the emulsion owns to water invasion in the porous media. These results demonstrated that the stability and plugging capacity of NS-DTAB system is much better relative to SDS system.

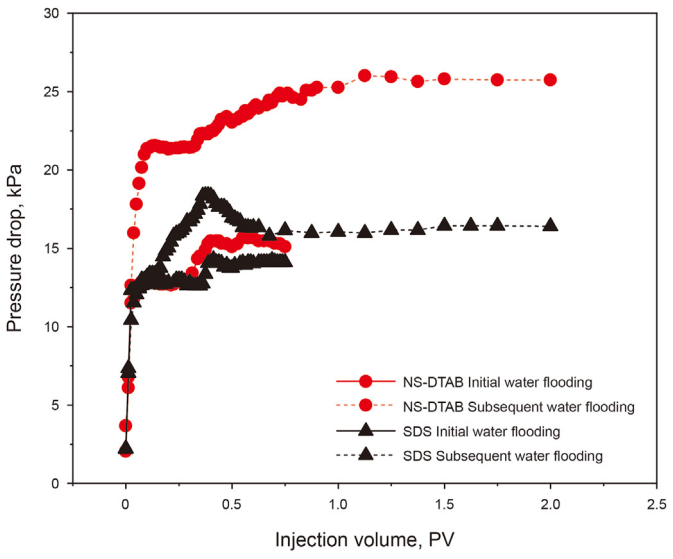


**Fig. 9.** Comparison of the pressure drop between different emulsifiers (8 mmol $L^{-1}$ SDS and 0.6 mmol $L^{-1}$ DTAB with 2 wt% NS) stabilized emulsion during initial and subsequent water flooding.

In addition, the results presented in Table 1 show that the incremental oil recovery of the sand pack (a) (injecting NSE) is higher than that of sand pack (b) (injecting SDS stabilized emulsion) during subsequent water flooding stage after the emulsion injection. The total oil recoveries of two sand packs are 80.71% and 69.42%, respectively. The results also indicated that the profile control ability of NSE is better than that of SDS emulsion and therefore, NSE could enhance more recovery of residual oil. The discussions above suggest that surface solidification which results from the adsorption of NS-DTAB complexes at oil-water interface plays a significant role to strengthen the emulsion stability.

## 4. Conclusion

In this study, a novel mechanism for diverting subsequent injected water of NSE was first proposed: adsorption of NS-DTAB complexes at oil-water interface could result in interface hardening, endowing the emulsion with a better stability and plugging ability. Different emulsion stabilizers including NS alone, DTAB alone and NS-DTAB complexes were investigated. Emulsion stabilized by mixture of DTAB and nano-silica displayed a satisfactory stability in both static and dynamic conditions. It is found that the adsorption of NS-DTAB complexes at oil-water interface can slow down the coalescence rate of droplets. Once the interface is jammed by DTAB-decorated nano-silica, the coalescences of droplets can be completely inhibited. What's more, in core flooding tests, emulsion stabilized by DTAB with nano-silica shows a powerful flow resistance to water invasion, which benefits the enhanced oil recovery.

## Acknowledgments

This work was supported by the National Natural Science Foundation of China (U1663206, 51704313), the Taishan Scholar Climbing Program in Shandong Province (tspd20161004) and the Fundamental Research Funds for the Central Universities (18CX02028A).

## Appendix A. Supplementary data

Supplementary data related to this article can be found at https://doi.org/10.1016/j.petsci.2021.11.001.

## References


Almobarky, M.A., AlYousef, Z., Schechter, D., 2017. A comparison between two anionic surfactants for mobility control of super critical $CO_2$ in foam-assisted miscible EOR. In: Carbon Management Technology Conference, July, Houston, Texas, USA. https://doi.org/10.7122/486486-MS.

Alvarez, N.J., Anna, S.L., Saigal, T., et al., 2012. Interfacial dynamics and rheology of polymer-grafted nanoparticles at air-water and xylene-water interfaces. Langmuir 28 (21), 8052–8063. https://doi.org/10.1021/la300737p.

Alyousef, Z.A., Almobarky, M.A., Schechter, D.S., 2018. The effect of nanoparticle aggregation on surfactant foam stability. J. Colloid Interface Sci. 511, 365–373. https://doi.org/10.1016/j.jcis.2017.09.051.

Aveyard, R., Binks, B.P., Clint, J.H., 2003. Emulsions stabilised solely by colloidal particles. Adv. Colloid Interface Sci. 100–2, 503–546. https://doi.org/10.1016/S0001-8686(02)00069-6.

Bai, B.J., Zhou, J., Yin, M.F., 2015. A comprehensive review of polyacrylamide polymer gels for conformance control. Petrol. Explor. Dev. 42 (4), 481–487 (in Chinese).

Bera, A., Kumar, T., Ojha, K., et al., 2013. Adsorption of surfactants on sand surface in enhanced oil recovery: isotherms, kinetics and thermodynamic studies. Appl. Surf. Sci. 284, 87–99. https://doi.org/10.1016/j.apsusc.2013.07.029.

Binks, B.P., Clint, J.H., 2002. Solid Wettability from surface energy components: relevance to pickering emulsions. Langmuir 18 (4), 1270–1273. https://doi.org/10.1021/la011420k.

Binks, B.P., Lumsdon, S.O., 2000. Influence of particle wettability on the type and stability of surfactant-free emulsions. Langmuir 16 (23), 8622–8631. https://doi.org/10.1021/la000189s.

Binks, B.P., Rodrigues, J.A., Frith, W.J., 2007. Synergistic interaction in emulsions stabilized by a mixture of silica nanoparticles and cationic surfactant. Langmuir 23 (7), 3626–3636. https://doi.org/10.1021/la0634600.

Binks, B.P., 2002. Particles as surfactants—similarities and differences. Curr. Opin. Colloid Interface Sci. 7 (1–2), 21–41. https://doi.org/10.1016/S1359-0294(02)00008-0.

Binks, B.P., 2001. Wetting: theory and experiment. Curr. Opin. Colloid Interface Sci. 6 (1), 17–21. https://doi.org/10.1016/S1359-0294(00)00094-7.

Caulfield, M.J., Qiao, G.G., Solomon, D.H., 2002. Some aspects of the properties and degradation of polyacrylamides. Chem. Rev. 33 (44), 274. https://doi.org/10.1002/chin.200244274.

Curschellas, C., Gunes, D.Z., Deyber, H., et al., 2012. Interfacial aspects of the stability of polyglycerol ester covered bubbles against coalescence. Soft Matter 8 (46), 11620–11631. https://doi.org/10.1039/C2SM26446C.

Dendukuri, D., Hatton, T.A., Doyle, P.S., 2007. Synthesis and self-assembly of amphiphilic polymeric microparticles. Langmuir 23 (8), 4669–4674. https://doi.org/10.1021/la062512i.

Du, K., Glogowski, E., Emrick, T., et al., 2010. Adsorption energy of nano- and microparticles at liquid-liquid interfaces. Langmuir 26 (15), 12518–12522. https://doi.org/10.1021/la100497h.

Forgiarini, A., Esquena, J., Gonzalez, C., et al., 2001. Formation of nano-emulsions by low-energy emulsification methods at constant temperature. Langmuir 17 (7), 2076–2083. https://doi.org/10.1021/la001362n.

Guo, F., Aryana, S., 2016. An experimental investigation of nanoparticle-stabilized CO2 foam used in enhanced oil recovery. Fuel 186, 430–442. https://doi.org/10.1016/j.fuel.2016.08.058.

Kong, X.L., Ohadi, M.M., 2010. Applications of micro and nano technologies in the oil and gas industry-Overview of the recent progress. In: Abu Dhabi International Petroleum Exhibition and Conference. UAE, November, Abu Dhabi. https://doi.org/10.2118/138241-MS.

Liu, X.B., Shi, S.W., Li, Y.N., et al., 2017. Liquid tubule formation and stabilization using cellulose nanocrystal surfactants. Angew. Chem. 56 (41), 12594–12598. https://doi.org/10.1002/anie.201706839.

Liu, Y.Z., Bai, B.J., Wang, Y.F., 2010. Applied technologies and prospects of conformance control treatments in China. Oil Gas Sci. Technol. 65 (6), 859–878. https://doi.org/10.2516/ogst/2009057.

Matteo, C., Candido, P., Vera, R., et al., 2012. Current and future nanotech applications in the oil industry. Am. J. Appl. Sci. 9 (6), 784–793. https://doi.org/10.3844/ajassp.2012.784.793.

McAuliffe, C.D., 1973. Oil-in-water emulsions and their flow properties in porous media. J. Petrol. Technol. 25 (6), 727–733. https://doi.org/10.2118/4369-PA.

Metin, C.O., Baran Jr., J.R., Nguyen, Q.P., 2012. Adsorption of surface functionalized silica nanoparticles onto mineral surfaces and decane/water interface. J. Nanoparticle Res. 14 (11), 1246. https://doi.org/10.1007/s11051-012-1246-1.

Paulson, O., Pugh, R.J., 1996. Flotation of inherently hydrophobic particles in aqueous solutions of inorganic electrolytes. Langmuir 12 (20), 4808–4813. https://doi.org/10.1021/la960128n.

Perino, A., Noik, C., Dalmazzone, C., 2013. Effect of fumed silica particles on water-in-crude oil emulsion: emulsion stability, interfacial properties, and contribution of crude oil fractions. Energy Fuels 27 (5), 2399–2412. https://doi.org/10.1021/ef301627e.

Pickering, S.U., 1907. CXCVI.-Emulsions. J. Chem. Soc. Trans. 91, 2001–2021. https://doi.org/10.1039/CT9079102001.

Ponce, F.R.V., Carvalho, M.S., Alvarado, V., 2014. Oil recovery modeling of macroemulsion flooding at low capillary number. J. Petrol. Sci. Eng. 119, 112–122. https://doi.org/10.1016/j.petrol.2014.04.020.

Saigal, T., Dong, H.C., Matyjaszewski, K., et al., 2010. Pickering emulsions stabilized by nanoparticles with thermally responsive grafted polymer brushes. Langmuir 26 (19), 15200–15209. https://doi.org/10.1021/la1027898.

Saikia, T., Sultan, A.S., 2020. Development of silane-modified colloidal silica pickering emulsion stabilized by organophilic micronized phyllosilicate for conformance control. J. Petrol. Sci. Eng. 194, 107427. https://doi.org/10.1016/j.petrol.2020.107427.

Samuelson, M.L., Constien, V.G., 1996. Effects of high temperature on polymer degradation and cleanup. In: SPE Annual Technical Conference and Exhibition. October, Denver, Colorado. https://doi.org/10.2118/36495-MS.

Sharma, T., Kumar, G.S., Chon, B.H., et al., 2014. Viscosity of the oil-in-water pickering emulsion stabilized by surfactant-polymer and nanoparticle-surfactant-polymer system. Korea Aust. Rheol. J. 26 (4), 377–387. https://doi.org/10.1007/s13367-014-0043-z.

Shi, S.L., Wang, L.S., Jin, Y.X., et al., 2014. Application progress and developmental tendency of emulsion system used in flooding, profile control and water plugging. Oilfield Chem. 31 (1), 141–145 (in Chinese).

Toor, A., Lamb, S., Helms, B.A., et al., 2018. Reconfigurable microfluidic droplets stabilized by nanoparticle surfactants. ACS Nano 12 (3), 2365–2372. https://doi.org/10.1021/acsnano.7b07635.

Walther, A., Müller, A.H.E., 2008. Janus particles. Soft Matter (4), 663–668. https://doi.org/10.1039/B718131K.

Wang, F.Q., Qu, Z.H., Kong, L.R., 2006. Experimental study on the mechanism of emulsion flooding with micromodels. Petrol. Explor. Dev. 33 (2), 221–224 (in Chinese).

Wang, H., Zhao, L., Song, G.L., et al., 2018. Organic-inorganic hybrid shell microencapsulated phase change materials prepared from $SiO_2$/TiC-stabilized pickering emulsion polymerization. Sol. Energy Mater. Sol. Cells 175, 102–110. https://doi.org/10.1016/j.solmat.2017.09.015.

Wu, Y.N., Chen, W.X., Dai, C.L., et al., 2017. Reducing surfactant adsorption on rock by silica nanoparticles for enhanced oil recovery. J. Petrol. Sci. Eng. 153, 283–287. https://doi.org/10.1016/j.petrol.2017.04.015.

Wu, Y.N., Fang, S.S., Zhang, K.Y., et al., 2018. Stability mechanism of nitrogen foam in porous media with silica nanoparticles modified by cationic surfactants. Langmuir 34 (27), 8015–8023. https://doi.org/10.1021/acs.langmuir.8b01187.

Wu, Y.N., Wang, R.Y., Dai, C.L., et al., 2019. Precisely tailoring bubble morphology in microchannel by nanoparticles self-assembly. Ind. Eng. Chem. Res. 58 (9), 3707–3713. https://doi.org/10.1021/acs.iecr.8b06057.

Xiao, J., Li, Y.Q., Huang, Q.R., 2016. Recent advances on food-grade particles stabilized Pickering emulsions: fabrication, characterization and research trends. Trends Food Sci. Technol. 55, 48–60. https://doi.org/10.1016/j.tifs.2016.05.010.

Yang, C.Z., 1985. The mechanism and methods of controlling surfactant losses in chemical flooding processes: Part 1. The mechanism. Oilfield Chem. 1, 9–20 (in Chinese).

Yin, G.N., Zheng, Z., Wang, H.T., et al., 2013. Preparation of graphene oxide coated polystyrene microspheres by pickering emulsion polymerization. J. Colloid Interface Sci. 394, 192–198. https://doi.org/10.1016/j.jcis.2012.11.024.

Yu, L., Ding, B.X., Dong, M.Z., et al., 2019. A new model of emulsion flow in porous media for conformance control. Fuel 241, 53–64. https://doi.org/10.1016/j.fuel.2018.12.014.

Yu, X.X., Wang, R.Y., Wu, Y.N., et al., 2019. The flow behaviors of nanoparticle-stabilized bubbles in microchannel: influence of surface hardening. AIChE J. 66 (4), e16865. https://doi.org/10.1002/aic.16865.

Zhao, G., Dai, C.L., Chen, A., et al., 2015. Experimental study and application of gels formed by nonionic polyacrylamide and phenolic resin for in-depth profile control. J. Petrol. Sci. Eng. 135, 552–560. https://doi.org/10.1016/j.petrol.2015.10.020.